CASL-U-2013-0220-000

Power uprates
and plant life extension

Consortium for Advanced Simulation of LWRs

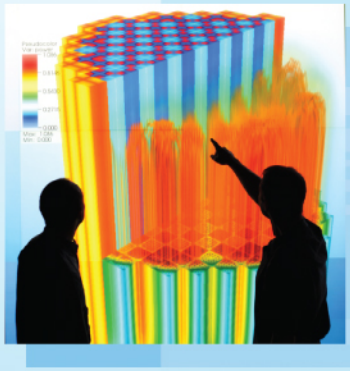

Engineering design
and analysis

L3:VUQ.VVDA.P5.02 Reducing Uncertainties via Predictive Modeling: FLICA4 Calibration using BFBT Benchmarks

Science-enabling
high performance
computing

Dan Cacuci, Erkan Arslan
North Carolina State University

May 5, 2013

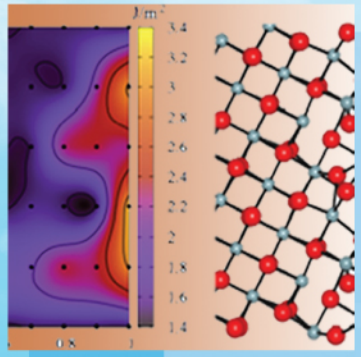

Fundamental science

Plant operational data

U.S. DEPARTMENT OF ENERGY | Nuclear Energy

Nuclear Science and Engineering: Submitted on May 5, 2013

REDUCING UNCERTAINTIES VIA PREDICTIVE MODELING: FLICA4 CALIBRATION USING BFBT BENCHMARKS

Dan G. Cacuci and Erkan Arslan

University of South Carolina, Department of Mechanical Engineering

300 Main Street, Columbia, SC 29208

Mail correspondence and page charges to Dr. Dan G. Cacuci (Cacuci@cec.sc.edu)

Abstract: This work applies the predictive modeling procedure formulated by Cacuci and Ionescu-Bujor (2010) to assimilate experimental data from the international OECD/NRC BWR Full Size Fine-Mesh Bundle Tests (BFBT) benchmarks to calibrate and reduce systematically and significantly the uncertainties in the predictions of the LWR thermal-hydraulics code FLICA4. The BFBT benchmarks were designed by the Nuclear Power Engineering Corporation (NUPEC) of Japan for enabling systematic validation of thermal-hydraulics codes by using full-scale experimental data. This work specifically uses BFBT experimental data for the "pump trip for a high-burnup assembly" in the predictive modeling formalism to calibrate parameters and time-dependent boundary conditions (power, mass flow rates, and outlet pressure distributions) in FLICA4, yielding best-estimate predictions of axial void fraction distributions. The resulting uncertainties for the best-estimate time-dependent model parameters and void fraction response distributions are shown to be smaller than the a priori experimental and computed uncertainties, thus demonstrating the successful use of predictive modeling for the large-scale reactor analysis code FLICA4 using BFBT benchmark-grade experiments.

I. INTRODUCTION

Gaining accurate knowledge about boiling transition and void fraction distribution is essential for the quantification of nuclear reactor safety margins. However, the theoretical principles underlying the numerical modeling of sub-channel void distribution are incompletely known, and the correlations replacing first-principles are not generally applicable to the wide range of geometrical arrangements and operating conditions found in operating LWRs of various types. From 1987 to 1995, the Nuclear Power Engineering Corporation of Japan (NUPEC) performed measurements[1,2] of void fraction distributions in full-size mock-up fuel bundles for both boiling water reactors (BWRs) and pressurized water reactors (PWRs). The void fraction distributions were visualized using computer tomography technology under actual plant conditions for mesh sizes smaller than a sub-channel. In addition to measuring void fraction distributions, NUPEC also performed steady state and transient measurement of critical power in equivalent full-size mock-ups. The NUPEC measurements are internationally considered to be highly reliable, thereby providing a comprehensive database for the development of consistent mechanistic models for predicting void fraction distributions and boiling transition in sub-channels. The international OECD/NRC BWR Full-Size Fine-Mesh Bundle Tests (BFBT) benchmarks[1,2] were established based on the NUPEC database to motivate research on insufficiently known two-phase flow regimes by facilitating a systematic comparison between full-scale experimental data and predictions of numerical simulation models. These benchmarks are particularly well suited for quantifying uncertainties in the prediction of detailed distributions of sub-channel void fractions and critical powers.

As is well known, nominal (or mean) values of experimentally measured or computed quantities are insufficient, by themselves, for applications; the quantitative uncertainties accompanying the measurements are also needed, along with the respective nominal (mean) values. Combination of data and theirs uncertainties requires reasoning from incomplete, error-afflicted, and occasionally discrepant

information for extracting "best estimate" values for model parameters and predicted results (responses), together with "best estimate" uncertainties for these parameters and responses.

Cacuci and Ionescu-Bujor[3,4] have proposed a comprehensive predictive modeling methodology for large-scale nonlinear time-dependent systems, enabling the reduction of uncertainties in best-estimate predictions following the combination ("assimilation") of experimental data with computational results (response sensitivities and propagated model parameter uncertainties). This predictive modeling methodology generalizes and significantly extends the results customarily used in nuclear engineering, as well as those underlying the so-called 4D-VAR data assimilation procedures in the geophysical sciences[5]. The predictive modeling methodology of Cacuci and Ionescu-Bujor[3,4] also provides quantitative indicators constructed from responses sensitivities (to model parameters) and covariance matrices (for measurements, as well as model parameters and responses) for determining the consistency (agreement or disagreement) among the a priori computational and experimental data (parameters and responses). Once the inconsistent data, if any, is discarded, this predictive modeling methodology yields best-estimate values for parameters and predicted responses, as well as best-estimate reduced uncertainties for (i.e., smaller values for the variances accompanying) the predicted best-estimate parameters and responses.

The above mentioned predictive modeling methodology has been successfully applied by Petruzzi et al[6] to a blow-down thermal-hydraulics benchmark of interest to nuclear reactor safety, demonstrating that the assimilation of consistent experimental data leads to a significant reduction of uncertainties of the best estimate predicted results. Going significantly beyond the scope of the work by Petruzzi et al[6], M.C Badea et al[7] applied the predictive modeling methodology of Cacuci and Ionescu-Bujor[3,4] to calibrate time-dependent model parameters and boundary conditions for the LWR core thermal-hydraulics code FLICA4[8] using the BFBT benchmark measurements for the "turbine trip without bypass BFBT test

number 4102-001~009", to obtain best-estimate predictions, with reduced uncertainties, for the following physical quantities: (i) pressure drops arising from steady one-dimensional FLICA4 simulations; (ii) axial void fractions distributions arising from transient one-dimensional FLICA4 simulations; and (iii) transversal void fraction distributions arising from steady three-dimensional FLICA4 simulations, at sub-channel level with cross-flows.

The present work continues the predictive modeling and validation of the thermal-hydraulics code FLICA4[8], by using the BFBT experimental benchmark "pump trip in a BWR for a high-burnup assembly". The experimental data for this benchmark is designated as "BFBT case 4102-001 ~ 027", and comprises the time-dependent record of the axial void distributions, at three elevations, in the BFBT test section containing a typical full-size (8x8) BWR-assembly subject to the "pump trip" design basis accident scenario. Section II of this work presents the salient predictive modeling formulas from the methodology of Cacuci and Ionescu-Bujor[3,4] for the predicted best-estimate responses and parameters, along with the corresponding predicted best-estimate covariances. These formulas are subsequently used in Section III in conjunction with the experimental data from the BFBT "pump trip, case 4102-001 ~ 027" benchmark to calibrate FLICA4 and produce best-estimate results, with reduced uncertainties, for the predicted void fraction distributions, as well as for the time-dependent power and mass flow distributions. Finally, Section IV summarizes the significance of this work and offers concluding remarks.

II. PREDICTIVE MODELING: SUMMARY OF FORMULAS FOR PREDICTING BEST-ESTIMATE MEANS AND COVARIANCES FOR MODEL PARAMETERS AND RESPONSES

Following the work of Cacuci and Ionescu-Bujor[3,4], the time-dependent physical system is considered to comprise N_α^κ model parameters and N_r^κ distinct responses, at every time node (step) $\kappa = 1, 2, \ldots, N_t$. Using superscripts to denote "time nodes" (or "steps"), the (column) vector $\boldsymbol{\alpha}^\kappa$ of N_α^κ model parameters, and the (column) vector $\mathbf{r}^\kappa$ of N_r^κ responses can be represented at every time node κ in component form as $\boldsymbol{\alpha}_\kappa = \left\{\alpha_{n_\kappa} \,|\, n = 1, \ldots N_{\alpha_\kappa}\right\}$, $\mathbf{r}_\kappa = \left\{r_{i_\kappa} \,|\, i = 1, \ldots, N_{r_\kappa}\right\}$, $\kappa = 1, \ldots, N_t$. At any time node κ, the system parameters are considered to be variates with known mean values $\left(\alpha_n^\kappa\right)^0, n = 1, \ldots N_\alpha^\kappa$, and known correlations between two parameters α_i^κ and $\alpha_j^\propto$, at two time nodes $\propto$ and κ; these correlations are denoted as

$$c_{\alpha,ij}^{\kappa\propto} \equiv \left\langle \left[\alpha_i^\kappa - \left(\alpha_i^\kappa\right)^0\right]\left[\alpha_j^\propto - \left(\alpha_j^\propto\right)^0\right]\right\rangle . \tag{1}$$

The above correlations constitute the elements of symmetric covariance matrices of the form

$$\mathbf{C}_\alpha^{\propto\kappa} \equiv \left\langle \left(\boldsymbol{\alpha} - \boldsymbol{\alpha}^0\right)^\propto \left[\left(\boldsymbol{\alpha} - \boldsymbol{\alpha}^0\right)^\kappa\right]^\dagger \right\rangle = \left(\mathbf{C}_\alpha^{\propto\kappa}\right)^\dagger = \mathbf{C}_\alpha^{\kappa\propto} = \left(\mathbf{C}_\alpha^{\kappa\propto}\right)^\dagger . \tag{2}$$

Similarly, the measured responses are characterized by mean values $\left(\mathbf{r}_m\right)^\kappa$ at a time node κ, and by symmetric covariance matrices between two time nodes $\propto$ and κ defined as

$$\mathbf{C}_m^{\propto\kappa} \equiv \left\langle \left(\mathbf{r} - \mathbf{r}_m\right)^\propto \left[\left(\mathbf{r} - \mathbf{r}_m\right)^\kappa\right]^\dagger \right\rangle = \left(\mathbf{C}_m^{\propto\kappa}\right)^\dagger = \mathbf{C}_m^{\kappa\propto} = \left(\mathbf{C}_m^{\kappa\propto}\right)^\dagger . \tag{3}$$

In general, the measured responses may be correlated to the parameters through response-parameter uncertainty matrices of the form

$$\mathbf{C}_{r\langle}^{\propto\langle} \;\alpha\; \left| \left(\mathbf{r} \square \mathbf{r}_m\right)^{\propto} \left[\left(\boldsymbol{\alpha} \square \boldsymbol{\alpha}^0\right)^{\langle}\right]^{\dagger} \right| \quad . \tag{4}$$

By using the maximum entropy principle in conjunction with Bayes' theorem, the methodology of Cacuci and Ionescu-Bujor[3,4] combines the a priori information presented in Eqs. (1) through (4) with the "likelihood" provided by the simulation model (in the present case: FLICA4) to yield expressions for the best-estimate predicted values for the model parameters and responses, along with corresponding reduced uncertainties (covariances), as follows:

1. Best-estimate predicted nominal values for the calibrated (adjusted) parameters:

$$\boldsymbol{\alpha}^{be} = \boldsymbol{\alpha}^0 + \left(\mathbf{C}_{\langle r} \square \mathbf{C}_{\langle} \left[\mathbf{S}\left(\boldsymbol{\alpha}^0\right)\right]^{\dagger}\right) \left[\mathbf{C}_d\left(\boldsymbol{\alpha}^0\right)\right]^{\square 1} \mathbf{d} \,. \tag{5}$$

In component form, the above expression for the calibrated best-estimate parameter values can be written in the form

$$\left(\boldsymbol{\alpha}^{be}\right)^{\langle} = \left(\boldsymbol{\alpha}^0\right)^{\langle} + \left[\int_{\propto=1}^{N_t} \left[\mathbf{C}_{\langle r}^{\langle\propto} \left[\sum_{\rangle=1}^{\propto} \mathbf{C}_{\langle}^{\langle\rangle} \left(\mathbf{S}^{\dagger}\right)^{\propto\rangle}\right]\right] \left[\sum_{|=1}^{N_t} \mathbf{K}_d^{\propto|} \mathbf{d}\right]\right], \quad \langle = 1, \ldots, N_t \,, \tag{6}$$

where $\mathbf{K}_d^{\langle|}$ denotes the corresponding $(\langle,|)$-element of the block-matrix $\mathbf{C}_d^{\square 1}$, with the block-matrix $\mathbf{C}_d\left(\boldsymbol{\alpha}^0\right)$ defined as follows:

$$\begin{aligned} \mathbf{C}_d\left(\boldsymbol{\alpha}^0\right) \alpha \left|\mathbf{d}\mathbf{d}^{\dagger}\right. &= \left(\mathbf{r}^{\mathrm{TM}} \square \mathbf{S}\left(\boldsymbol{\alpha}^0\right)^{\mathrm{TM}} \boldsymbol{\alpha}\right)\left(\mathbf{r}^{\dagger} \square \mathbf{r}^{\mathrm{TM}} \boldsymbol{\alpha}^{\dagger} \left[\mathbf{S}\left(\boldsymbol{\alpha}^0\right)\right]^{\dagger}\right) \\ &= \mathbf{C}\left(\boldsymbol{\alpha}^0\right) \square \mathbf{C}\left[\mathbf{S}\left(\boldsymbol{\alpha}^0\right)\right]^{\dagger} \square \left[\mathbf{S}\left(\boldsymbol{\alpha}^0\right)\right] \mathbf{C} + \mathbf{C} \,. \end{aligned} \tag{7}$$

$rc\left(\quad\right) \quad r\langle \square \left(\quad\right)\rfloor \quad \square\left(\quad\right)\rfloor \langle r \quad m$

In the above (and subsequent) expressions, the superscript "†" denotes "transposition". The block-matrix $\mathbf{S}$ that appears in the above expressions is defined as

$$\mathbf{S} \propto \begin{pmatrix} \mathbf{S}^{11} & \cdots & \mathbf{0} \\ \vdots & \ddots & \vdots \\ \mathbf{S}^{N_t 1} & \cdots & \mathbf{S}^{N_t N_t} \end{pmatrix}, \tag{8}$$

comprising $\left(J_r^{\prime} - J_{\langle}^{\propto}\right)$-dimensional matrix components $\mathbf{S}^{\prime\propto}$, $1 \delta \propto \delta \prime$, defined as

$$\mathbf{S}^{\prime\propto} \begin{pmatrix} \mathbf{p}^{\propto} \\ 0 \end{pmatrix} = \begin{pmatrix} s_{11}^{\prime\propto} & \cdots & s_{1N}^{\prime\propto} \\ \vdots & s_{in}^{\prime\propto} & \vdots \\ s_{I1}^{\prime\propto} & \cdots & s_{IN}^{\prime\propto} \end{pmatrix} = \begin{pmatrix} \frac{\square R_1^{\prime}}{\square \langle_1^{\propto}} & \cdots & \frac{\square R_1^{\prime}}{\square \langle_N^{\propto}} \\ \vdots & \frac{\square^{\prime}}{R_i} & \vdots \\ \frac{\square R_I^{\prime}}{\square \langle_1^{\propto}} & \cdots & \frac{\square R_I^{\prime}}{\square \langle_N^{\propto}} \end{pmatrix}, \quad 1 \delta \propto \delta \prime, \tag{9}$$

where the elements $\square R_i^{\prime} \blacksquare \square \langle_n^{\propto}$ represent the first Gateaux-derivatives of a computed response $R_i^{\prime}$ with respect to a model parameter $\langle_n^{\propto}$.

The covariance matrix $\mathbf{C}_{rc}$ appearing in Eq.(7) is a symmetric block-matrix that denotes the covariances of the computed responses, and is defined as follows:

$$\mathbf{C}_{rc} \propto \begin{pmatrix} \mathbf{C}_{rc}^{11} & \cdots & \mathbf{C}_{rc}^{1N_t} \\ \vdots & \ddots & \vdots \\ \mathbf{C}_{rc}^{N_t 1} & \cdots & \mathbf{C}_{rc}^{N_t N_t} \end{pmatrix}; \qquad \mathbf{C}_{rc}^{\prime\propto} = \prod_{|=1}^{\prime} \prod_{\rangle=1}^{\propto} \mathbf{S}^{\prime|} \mathbf{C}_{\langle}^{|\rangle} \left(\mathbf{S}^{\propto\rangle}\right)^{\dagger} = \left(\mathbf{C}_{rc}^{\propto\prime}\right)^{\dagger}; \qquad \prime, \propto = 1, \ldots, N_t. \tag{10}$$

The vector $\mathbf{d}$, which first appears in Eq. (5), denotes the vector of "deviations" reflecting the discrepancies between the nominally computed responses and the corresponding nominal values of the

measured responses, and is defined as

$$\mathbf{d} \propto \mathbf{R}\left(\boldsymbol{\alpha}^{0}\right) - \mathbf{r}_{m} \tag{11}$$

2. The best-estimate predicted nominal values for the calibrated (adjusted) responses:

$$\mathbf{r}\left(\boldsymbol{\alpha}^{be}\right) = \mathbf{r}_{m} + \left(\mathbf{C}_{m} - \mathbf{C}_{r\alpha}\left[\mathbf{S}\left(\boldsymbol{\alpha}^{0}\right)\right]^{\dagger}\right)\left[\mathbf{C}_{d}\left(\boldsymbol{\alpha}^{0}\right)\right]^{-1}\mathbf{d}\,. \tag{12}$$

At a specific time node α, each component $\left(\mathbf{r}^{be}\right)^{\alpha}$ of $\mathbf{r}\left(\boldsymbol{\alpha}^{be}\right)$ has the explicit form

$$\left(\mathbf{r}^{be}\right)^{\alpha} = \left(\mathbf{r}_{m}\right)^{\alpha} + \sum_{\beta=1}^{N_t}\left[\left(\mathbf{C}_{m}^{\alpha\beta} - \sum_{\gamma=1}^{N_t}\mathbf{C}_{r\alpha}^{\alpha\gamma}\left(\mathbf{S}^{\dagger}\right)^{\gamma\beta}\right)\left[\sum_{\delta=1}^{N_t}\mathbf{K}_{d}^{\beta\delta}\mathbf{d}^{\delta}\right]\right], \quad \alpha = 1,\ldots,N_t\,. \tag{13}$$

3. The expressions for the predicted best-estimate covariances $\mathbf{C}_{\alpha\beta}^{be}$ and $\mathbf{C}_{r}^{be}$ corresponding to the best-estimate parameters $\boldsymbol{\alpha}^{be}$ and responses $\mathbf{r}\left(\boldsymbol{\alpha}^{be}\right)$, respectively, together with the predicted best-estimate parameter-response covariance matrix $\mathbf{C}_{\alpha r}^{be}$. The block-matrix components, which correlate two (distinct or not) time-nodes, of these calibrated best-estimate covariance matrices are given below:

$$\left(\mathbf{C}^{be}\right)^{\alpha\beta} = \mathbf{C}^{\alpha\beta} - \sum_{\gamma=1}^{N_t}\sum_{\delta=1}^{N_t}\left[\mathbf{C}^{\alpha\gamma} - \mathbf{C}^{\alpha\delta}\left(\mathbf{S}^{\dagger}\right)^{\gamma\delta}\right]\mathbf{K}_{d}^{\gamma\delta}\left[\mathbf{C}^{\delta\beta} - \mathbf{S}^{\delta\gamma}\mathbf{C}^{\gamma\beta}\right], \tag{14}$$

$$\left(\mathbf{C}^{be}\right)^{r\alpha} = \mathbf{C}^{r\alpha} - \sum_{\gamma=1}^{N_t}\sum_{\delta=1}^{N_t}\left[\mathbf{C}^{\alpha\gamma} - \mathbf{C}^{\alpha\delta}\left(\mathbf{S}^{\dagger}\right)^{\gamma\delta}\right]\mathbf{K}_{d}^{\gamma\delta}\left[\mathbf{C}^{\delta\beta} - \mathbf{S}^{\delta\gamma}\mathbf{C}^{\gamma\beta}\right], \tag{15}$$

$$\left(\mathbf{C}^{be}\right)^{r\alpha} = \mathbf{C}^{r\alpha} - \sum_{\gamma=1}^{N_t}\sum_{\delta=1}^{N_t}\left[\mathbf{C}^{\alpha\gamma} - \mathbf{C}^{\alpha\delta}\left(\mathbf{S}^{\dagger}\right)^{\gamma\delta}\right]\mathbf{K}_{d}^{\gamma\delta}\left[\mathbf{C}^{\delta\beta} - \mathbf{S}^{\delta\gamma}\mathbf{C}^{\gamma\beta}\right]. \tag{16}$$

The methodology of Cacuci and Ionescu-Bujor[3,4] also provides the consistency indicator

$$\chi^2 \propto \mathbf{d}^{\dagger} \left[\mathbf{C}_d \left(\boldsymbol{\alpha}^0 \right) \right]^{-1} \mathbf{d} . \tag{17}$$

As the above expression indicates, the indicator χ^2 represents the square of the length of the vector $\mathbf{d}$, measuring (in the corresponding metric) the deviations between the experimental and nominally computed responses. Note that χ^2 can be evaluated directly from the originally given data (i.e., given parameters and responses, together with their original uncertainties), once the response sensitivities have been computed by either forward or adjoint methods[9]. Recall that the χ^2 (chi-square) distribution with n degrees of freedom of the continuous variable x, $0 \le x < \infty$ is defined as

$$P\left(x < \chi^2 < x + dx \right) = k_n(x)\,dx = \frac{1}{2^{n/2}\,\Gamma\left(n/2\right)} x^{n/2-1} e^{-x/2} dx, \; x > 0, \; \left(n = 1, 2, \ldots \right). \tag{18}$$

The χ^2- distribution is a measure of the deviation of a “true distribution” (in this case – the distribution of experimental responses) from the hypothetic one (in this case – a Gaussian). The mean and variance of x are $\langle x \rangle = n$ and $\mathrm{var}(x) = 2n$. As the dimension of $\mathbf{d}$ indicates, the number n of degrees of freedom characteristic of the calibration under consideration is equal to the number of experimental responses, i.e., $n = \sum_{r=1}^{N_t} N_r$. The value of χ^2 computed using Eq. (18) provides a very valuable quantitative indicator for investigating the agreement between the computed and experimental responses, measuring essentially the consistency of the experimental responses with the model parameters.

III. FLICA4 PREDICTIVE MODELING OF THE PUMP-TRIP NUPEC BFBT BENCHMARK EXPERIMENT

III.A Description of the BFBT "Pump-Trip High-Burnup" Experiment

The BFBT facility is limited to a maximum pressure of 10.3 MPa, a temperature of 315°C, a power of 12 MW, and a maximum mass flow of 20.83 kg/s. The coolant circulation is ensured by a pump, and the amount of coolant required by a specific experiment is regulated by valves that are located directly behind the pump filter. To avoid thermal shocks, the single-phase coolant is pre-heated in the inlet section. For the various BFBT experiments, corresponding two-phase flow conditions are provided inside the test section by the electrically heated rods in the mock-up BWR test assembly, which is contained inside a pressure vessel. The BFBT experimental benchmark "pump trip in a high burnup BWR assembly" has been selected in this work in order to calibrate the core thermal-hydraulics code FLICA4[7]. The experimental data for this benchmark is designated as "case 4102-001 ~ 027", comprising the time-dependent record of the axial void distributions, at three elevations, in a mock-up of a typical 8x8 BWR assembly. Figure 1 indicates the three elevations (at 682 mm, 1706 mm, and 2730 mm, from bottom to top) at which the void fraction responses R_1, R_2 and R_3 were measured. Figure 2 depicts the cross-sectional view of the BWR assembly. The typical power distribution in an actual BWR assembly is simulated using electrically heated rods. The various numbers in Figure 2 indicate various power peaking factors, which are specified in Table 1. The boundary conditions imposed on the test section are shown in Figure 3, and represent actual operating conditions for a typical BWR for the so-called "high-burnup case".

Group number	Group type	Power Peaking Factor
1	Heater	1.30
2	Heater	1.15
3	Heater	0.89
4	Heater	0.45
5	Water tube	0.00

Table 1: Power peaking factors for the "pump trip high burnup" assembly

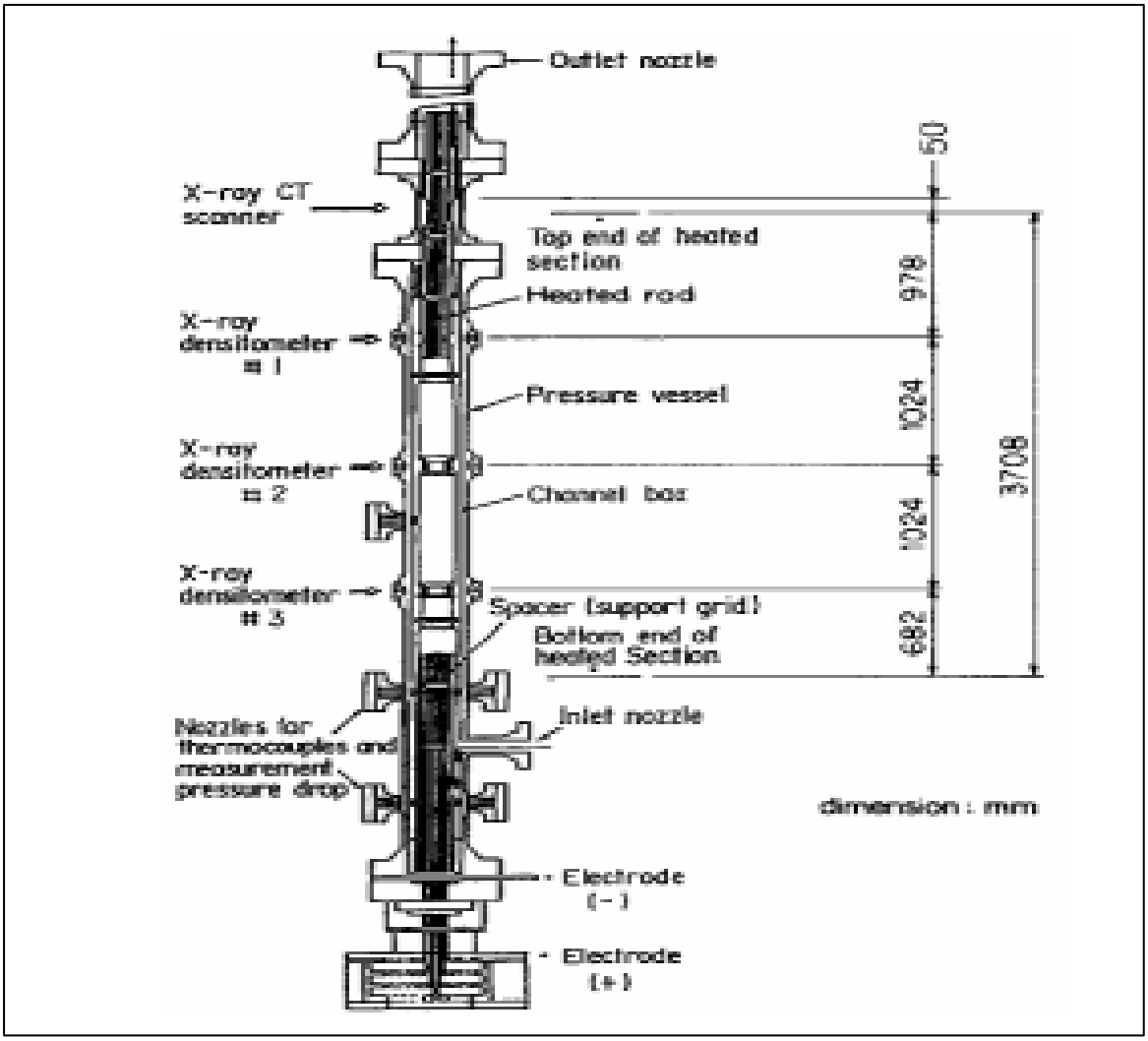

Figure 1: BFBT Test Section

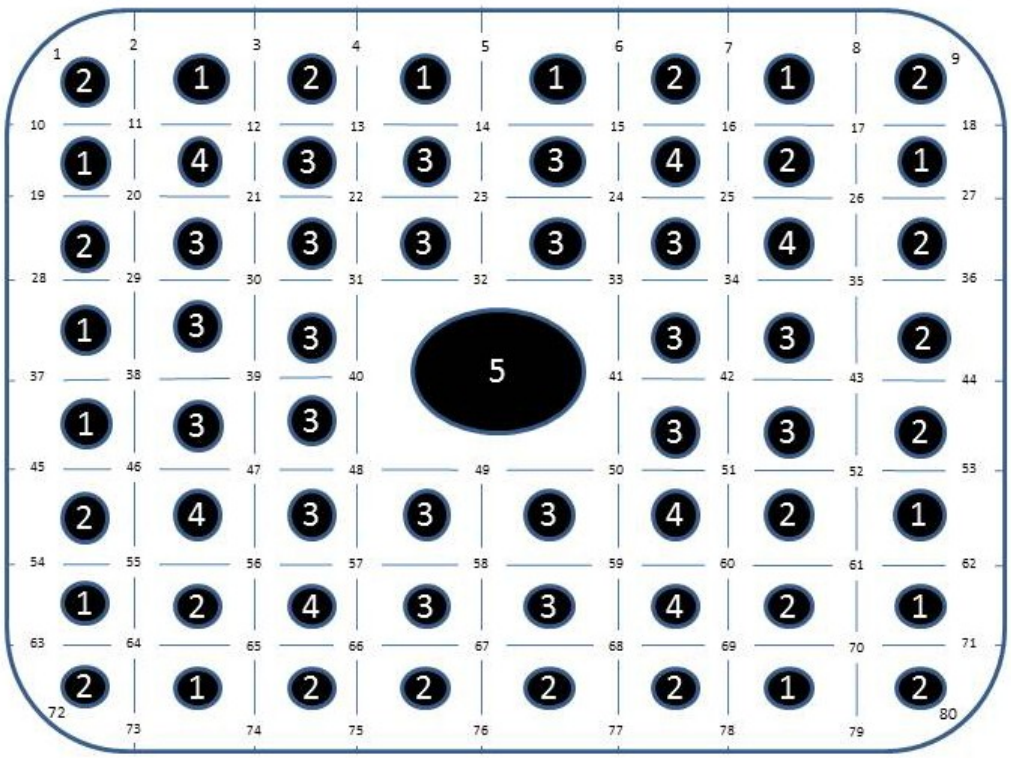

Figure 2: Cross sectional view of BWR mock-up assembly

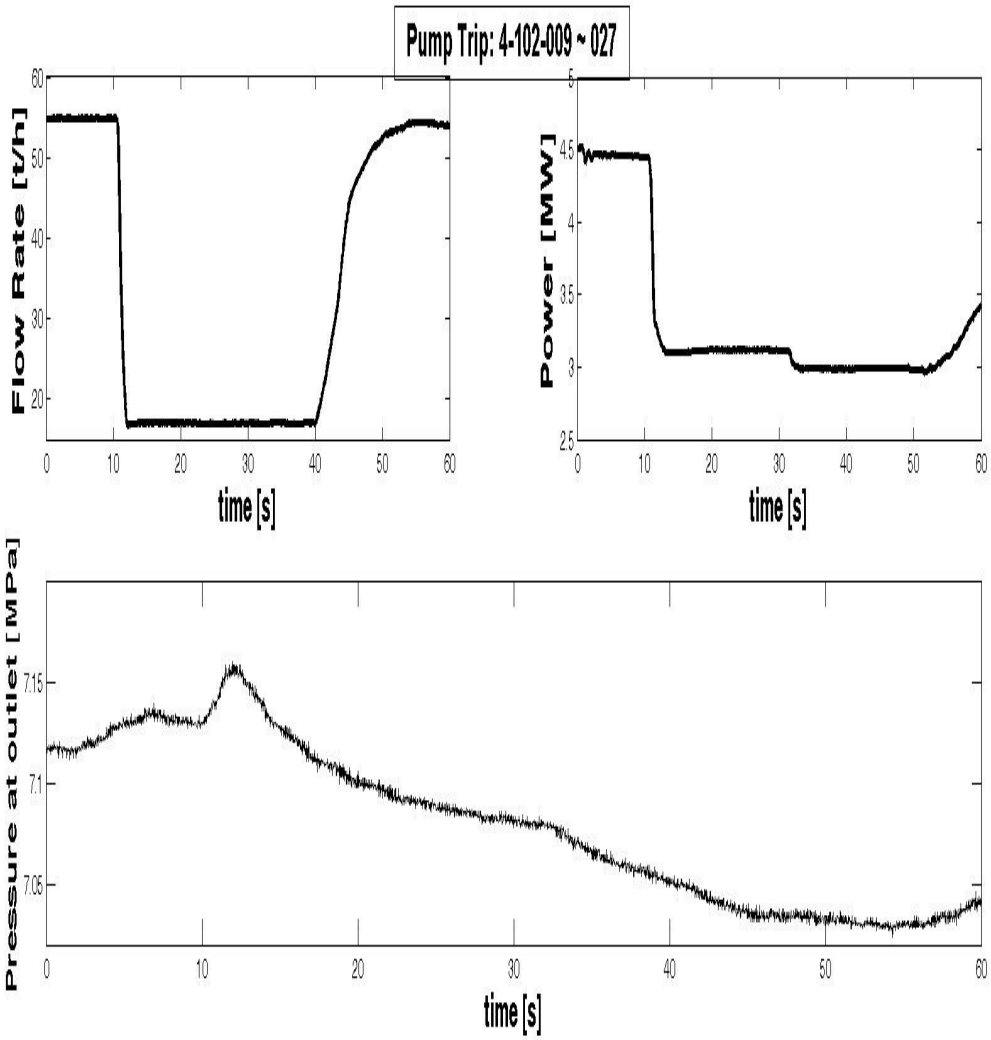

Figure 3: Time-dependent (experimentally measured) boundary conditions for the mass flow rate (top left), power distribution (top right) and the outlet pressure (bottom)

III.B. Predictive Modeling Using FLICA4

The predictive modeling formulas presented in Section II were used in conjunction with experimental measurements of void fractions (at the three levels indicated in Figure 1) together with the following FLICA4 time-dependent parameters: mass-flow, power-distribution and outlet pressure. The values of the time-dependent parameters mass-flow, the power-distribution and the outlet pressure were extracted from the corresponding data set (i.e., the case 4-102-009~027" of the BFBT benchmark) at every 100 milliseconds, for a total of 1800 values during the 60 seconds of the considered pump-trip transient. The relative standard deviations for the mass flow rate, power distribution and outlet pressure were 1.5%, 1.5%, and 1%, respectively; these measurements were considered to be uncorrelated in time.

As shown in Figure 1, the void fraction distributions were measured at three different axial positions: 2703 mm, 1706 mm, and 682 mm. These experimental measurements, together with their standard deviations, are depicted in Figure 4: the data at 2703 mm is labeled R_1, the data at 1706 mm is labeled R_2 and the data at 682 mm is labeled R_3. In the absence of information to the contrary, these experimentally measured responses were considered to be uncorrelated, and their relative standard deviations were estimated to be 5%. Figure 4 also depicts, using dashed-lines, the nominal values of the void fractions computed using FLICA4. For these computations, the test section, including the BWR assembly, were modeled by using a CAD representation involving a uniform hexahedral discretization with 1000 axial sub-divisions. This discretization makes it possible to determine accurately the void distribution at the measurement levels within a reasonable computational time. As Figure 4 indicates, the FLICA4 results seem to be consistent with the measurements during the period between 15 seconds and 45 seconds, but appear to be inconsistent with the measurement at the start of the transient (until about 15 seconds into

the transient) and at the end of the transient, beyond 45 seconds. The results presented in Figure 2 also indicate that the FLICA4 computations are more consistent with the measurements at high values of the void fraction (i.e., for the responses R_1 and R_2) but are systematically lower than the measurements for low values of the void fractions (i.e., for response R_3).

A total of 1530 experimental responses (specifically: 510 void fraction values measured at every 100 milliseconds at each of the three measuring levels, commencing at 9 seconds after the start of the transient, for a period of 60 seconds) were used in the predictive modeling formulas presented in Section II for calibrating FLICA4. The sensitivities of each of these 1530 responses to the FLICA4 time-dependent model parameters (power, mass flow rate, and outlet pressure) were computed by finite differences using forward FLICA4-computatioms, since FLICA4 does not have an adjoint model suitable for computing response sensitivities efficiently.

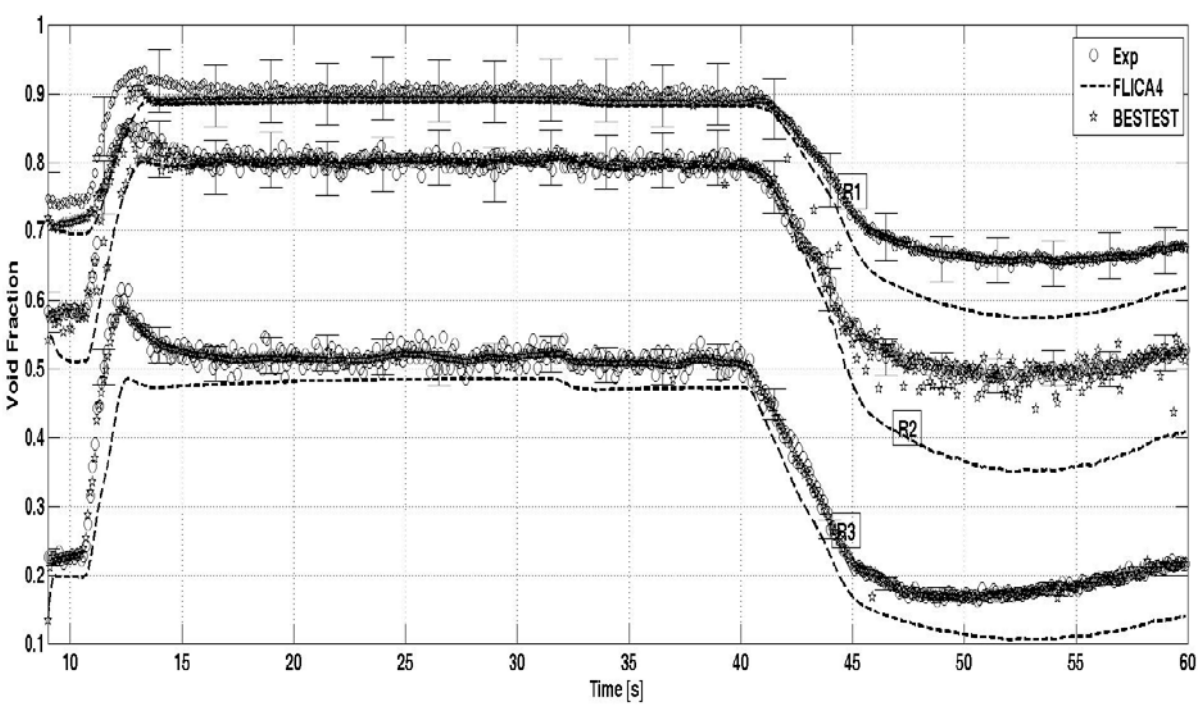

Figure 4: Experimental records (circles), FLICA4 results (dashed lines), and predicted best-estimate mean values for the void fraction responses (stars)

The computational and experimental responses shown in Figure 4 have been combined ("data assimilation") using the formulas presented in Section II to obtain best-estimate predicted responses, parameters, and corresponding reduced uncertainties. The predicted best-estimate mean-values of the responses are also shown (depicted by "starts") in Figure 4; the predictive modeling formula shown in Eq. (14) has significantly improved the predicted mean-values of the void fractions, making the predictions practically indistinguishable from the experimental values.

The top plot in Figure 5 presents the FLICA4-computed response uncertainties (± 1standard deviation computed using Eq. (11), around the computed nominal values presented in Figure 4). These uncertainties underscore the discrepancies between the experimental measurements and the FLICA4 computations for high void fractions, both for early and late times into the pump-trip transient. These discrepancies are caused by numerical instabilities in FLICA4 stemming from the rapid changes in the boundary conditions --especially the pressure. On the other hand, the bottom plot in Figure 5 presents the *predicted best-estimate responses*, computed with Eq. (14), together with the *predicted one-standard deviation* upper- (UUB) and, respectively, lower-uncertainty (LUB) bounds, computed using Eq. (16). These plots underscore the very significant improvement in the predicted responses, which have become almost indistinguishable from the experimental values for all three responses, for the majority of the duration of the transient. The only discrepancies between the predicted best-estimate values and the experiments remain for the last 5 seconds of the transient for the response R_1, at high void fraction values. The suppression of numerical instabilities following the data assimilation and model calibration of the time-dependent boundary conditions (also to be discussed in conjunction with the results depicted in Figures 5 and 6) in FLICA4 is underscored by the good agreement that can be visually observed in

Figure 5 (bottom) between the measured and predicted responses R_2 and R_3. The visual impression indicated by Figure 5 (bottom), namely of barely consistent agreement between the experimental and predicted void fractions for the high void fraction responses R_1, but very good agreement for the measured and predicted void fractions responses R_2 and R_3, is confirmed by the numerical values of the "chi-square-like consistency indicators" presented in Eq. (18) , which were found to have the following values: $\chi_1^2 / N_R = 0.53 < 1.0$ for the $N_R = 510$ degrees of freedom (measurements) for the response R_1; $\chi_2^2 / N_R = 1.02 \approx 1.0$ for the $N_R = 510$ measurements R_2; and $\chi_3^2 / N_R = 1.01 \approx 1.0$ the $N_R = 510$ measurements R_3. Note that although the off-diagonal (a posteriori response-response) correlation terms in the matrices $\left(\mathbf{C}_r^{be}\right)^{\chi^2}$, computed using Eq. (15), are non-zero, they are inconsequential, being all less than 1%. Similarly, computing the matrix $\left(\mathbf{C}_{r\zeta}^{be}\right)^{\chi^2}$ using Eq. (16) yields non-zero, but very small (all less than 1%) --and hence inconsequential-- a posteriori parameter-response correlations. Therefore, these correlation terms are not presented here.

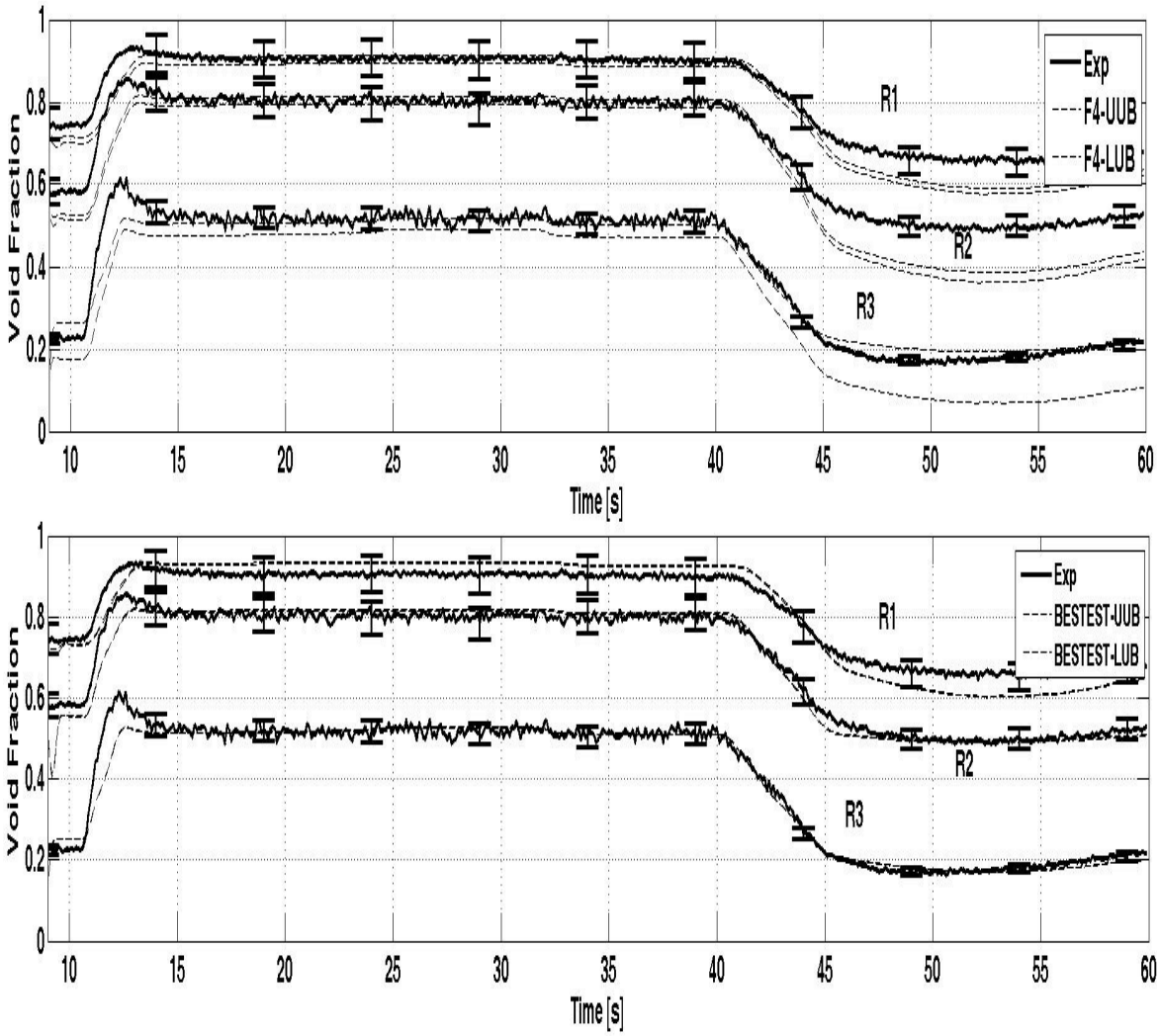

Figure 5: Experimental records (continuous lines), FLICA4-computed (± 1) standard deviations (top), and predicted best-estimate (± 1) standard deviations (bottom)

The predicted time-dependent best-estimate mass flow rate and power distribution, computed using Eq. (7), together with their accompanying predicted (± 1) standard-deviations computed using Eq. (15), are shown in Figures 6 and 7. Both figures indicate that the predictive modeling procedure performs very well, practically "overlaying" the predicted values over the experimentally determined ones, reducing the experimental uncertainties even further. As shown in Figures 5 and 6, the predicted a posteriori

parameter (± 1) standard-deviations are very small (less than 2%). These a posteriori standard deviations were computed by using Eq. (14); of course these computations yielded the complete matrices $\left(\mathbf{C}_{\langle}^{be}\right)^{\{\propto}$, not just the variances (diagonal terms). However, although these off-diagonal terms in $\left(\mathbf{C}_{\langle}^{be}\right)^{\{\propto}$ --namely the a posteriori parameter-parameter correlations-- were non-zero, they were inconsequential, being all less than 1%; therefore, these a posteriori parameter-parameter correlations are not presented here.

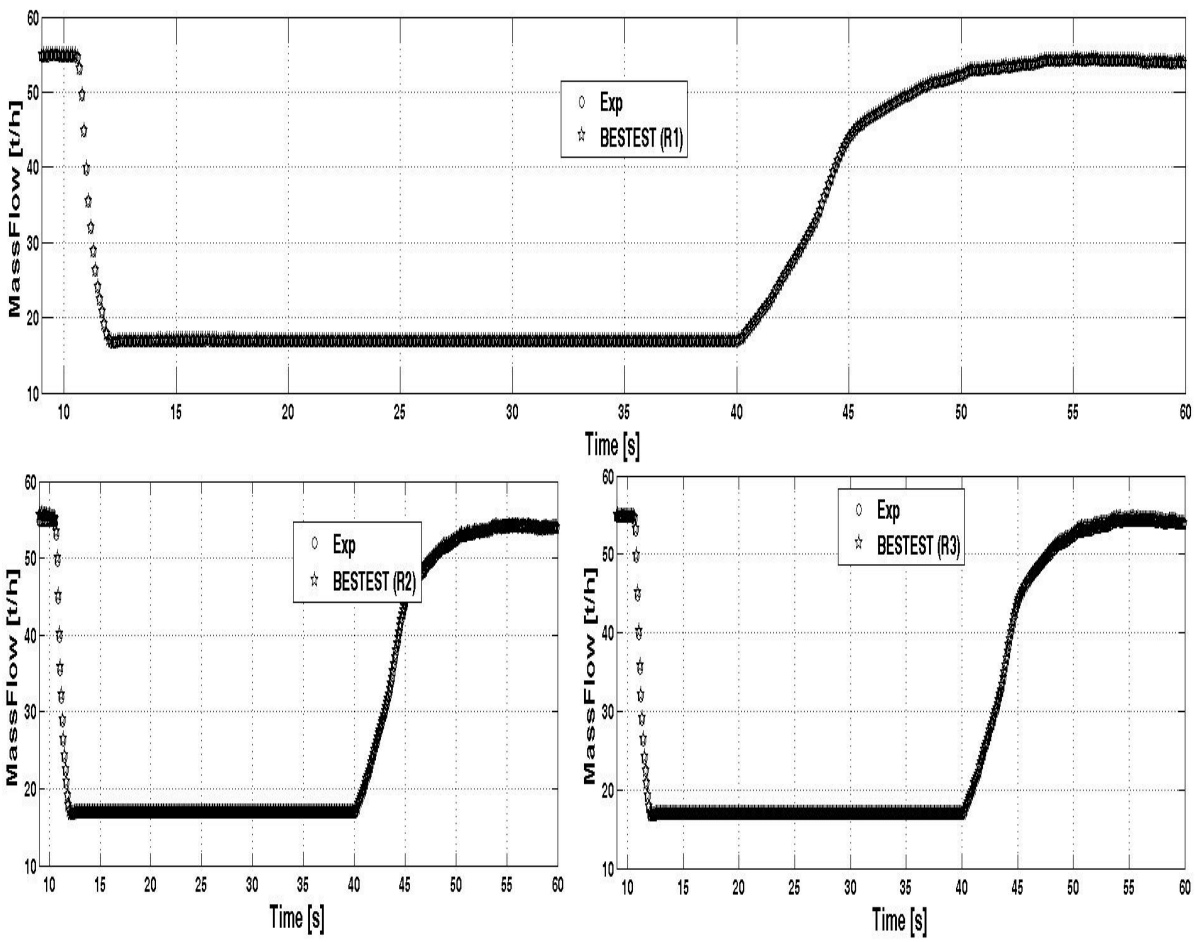

Figure 6: Experimental (circles) and best-estimated (stars) mass flow parameters of the R1, R2 and R3 response for the FLICA4 time-dependent parameters

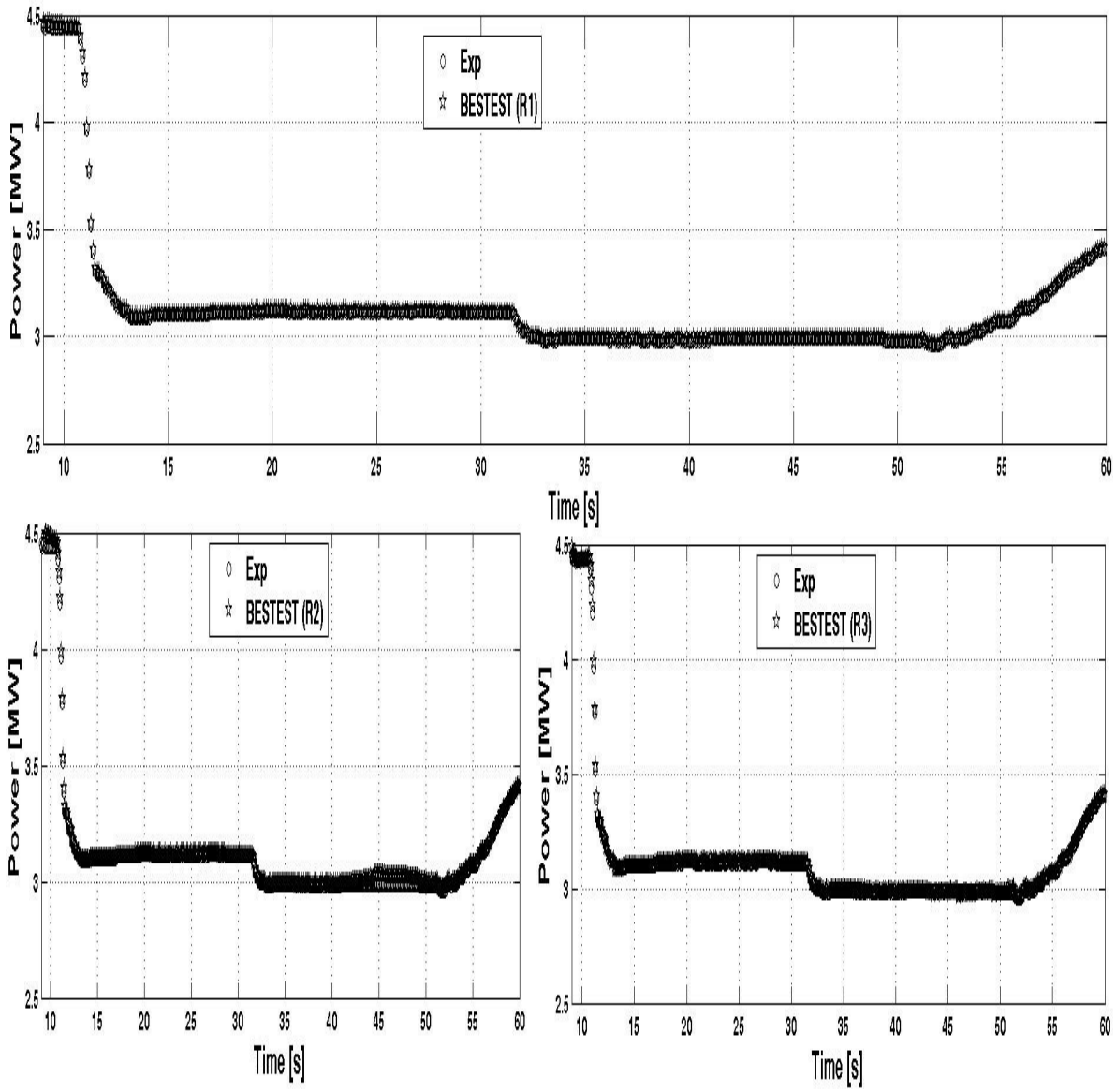

Figure 7: Experimental (circles) and best-estimated (stars) power distribution of the R1, R2 and R3 response for the FLICA4 time-dependent parameters

IV. SUMMARY AND CONCLUSIONS

This work has presented a large-scale application of the predictive modeling methodology proposed by Cacuci and Ionescu-Bujor[3,4] to the three-dimensional thermal-hydraulics code FLICA4[8], which is routinely used for the analysis and design of light-water reactors (LWR). This work continues the initial predictive modeling work reported by M.C. Badea et al[7], which used the BFBT benchmark measurements from the experiment "turbine trip without bypass" for predictive modeling using FLICA4, for the following benchmark measurements: (i) pressure drops (steady one-dimensional simulations); (ii) axial void fractions distributions (transient one-dimensional simulations); and (iii) transversal void fraction distributions (steady three-dimensional simulations, at sub-channel level with cross-flows). The predictive modeling results presented in this work follow the assimilation of experimental data from the OECD/NRC BWR Full-Size Fine-Mesh Bundle Tests (BFBT) benchmarks "pump trip at high burnup," and clearly demonstrate that assimilation of consistent information leads to more precisely predicted, reducing the accompanying uncertainties, often by large factors. The predictive modeling's quantitative "chi-square-like" indicator takes on values close to unity, indicating that the computations are consistent with the measurements.

The predictive modeling formulas in this work use first-order response sensitivities only. Nevertheless, model response nonlinearities can be taken into account by iterative applications of these formulas, in the spirit of incomplete Newton methods that do not use Hessian information. This strategy results in considerable savings of computational memory, which is a very important consideration when dealing with large-scale realistic physical systems. The development of higher-order predictive modeling formalisms is very important not only for enabling the quantification of the impact of higher-order

sensitivities and correlations, but also for quantifying non-Gaussian features (e.g., asymmetries, importance of tails) of the posterior joint distribution of computations and experiments, and is therefore an important objective of ongoing research.

Acknowledgement

The research of Erkan Arslan was partially supported by the Consortium for Advanced Simulation of Light Water Reactors (http://www.casl.gov), an Energy Innovation Hub (http://www.energy.gov/hubs) for Modeling and Simulation of Nuclear Reactors under U.S. Department of Energy Contract No. DE-AC05-00OR22725.

REFERENCES

1. H. Utsuno, K. Fumio, "NUPEC BWR FULL SIZE FINE MESH BUNDLE TEST (BFBT) BENCHMARK," Nuclear Engineering Program, Japan Nuclear Energy Safety Organization, Japan (2005).

2. B. Neykov, F. Aydogan, L. Hochreiter, K. IIanov, 2005, "NUPEC BWR FULL SIZE FINE MESH BUNDLE TEST (BFBT) BENCHMARK," Nuclear Engineering Program, Pennsylvania State University (2005).

3. D.G. Cacuci and M. Ionescu-Bujor, "Best Estimate Model Calibration and Prediction through Experimental Data Assimilation: Mathematical Framework", *Nucl. Sci. & Eng*., **165**, 18-44 (2010).

4. D.G. Cacuci and Mihaela Ionescu-Bujor, "Sensitivity and Uncertainty Analysis, Data Assimilation and Predictive Best-Estimate Model Calibration", Chapter 17 in Vol.3, pp 1913 – 2051, *Handbook of Nuclear Engineering*, D. G. Cacuci, Editor, ISBN: 978-0-387-98150-5, Springer New York / Berlin, 2010.

5. W. Lahoz, B. Khattatov, and R. Ménard, Editors, "Data Assimilation: Making Sense of Observations", Springer Verlag, 2010.

6. A. Petruzzi, D. G. Cacuci, and F. D'Auria, "Best-Estimate Model Calibration and Prediction Through Experimental Data Assimilation: Application to a Blowdown Benchmark Experiment", *Nucl. Sci. Eng*., **165**, 45-100, 2010.

7. M. C. Badea, D.G. Cacuci, and A.F. Badea, "Best-Estimate Predictions and Model Calibration for Reactor Thermal-Hydraulics", *Nucl. Sci. Eng.*, **172**, 1-19, 2012.

8. Ph. Fillion et al.: "FLICA4 Reference manual of modules and procedures", User Guide Version V1.10.1, CEA (2007).

9. D.G. Cacuci, *Sensitivity and Uncertainty Analysis: Theory*, **Vol. I,** Chapman & Hall/CRC, (2003).